Electronic Supplementary Material (ESI) for Lab on a Chip.

Supplementary information

Microfluidic Particle Counter Visualizing Mucosal Antibody Levels against SARS-CoV-2 in the Upper Respiratory Tract for Rapid Evaluation of Immune Protection

Authors

Jiaheng Li[a], Lok Ting Chu[b], Hogi Hartanto[a], Guihuan Guo[a], Lu Liu[a], Jianpeng Wu[a], Minghui Wu[a], Chenyu Cui[a], Gaobo Wang[a], Wengang Liu[a], Hoi Kwan Kwong[a], Siying Wu[a], and Ting-Hsuan Chen[a,c,d,*].

Affiliations

[a]Department of Biomedical Engineering, City University of Hong Kong, Kowloon, Hong Kong SAR, China.

[b]Department of Biochemistry and Molecular Biology, School of Basic Medical Sciences, Guang Dong Medical University, Zhanjiang, China.

[c]City University of Hong Kong Shenzhen Research Institute, Shenzhen, China.

[d]Hong Kong Centre for Cerebro-cardiovascular Health Engineering, Hong Kong Science Park, Hong Kong SAR, China.

[*]Corresponding Author. Email: thchen@cityu.edu.hk.

1. Methods and materials

1.1 Reagents and materials

In the microparticle system, carboxyl MMPs (catalog no. PMC3HP, 11653, 3.06 μm in diameter, ～1.4 g/cc - 1.8 g/cc) and carboxyl PMPs (catalog no. PC07002, 12793, 15.3 μm in diameter, ～1.05 g/cc - 1.1 g/cc) were purchased from Bangs Laboratories Inc., USA. Powder of 1-Ethyl-3-(3-dimethylaminopropyl) carbodiimide hydrochloride (EDC), N-hydroxysuccinimide (NHS) and Dulbecco's phosphate-buffered saline (DPBS), goat anti-human IgG (H+L) antibody (catalog no. A18813), blocker casein (catalog no. 37582) were purchased from Thermo Fisher Scientific, USA. 2-(N-morpholino) ethane-sulfonic acid (MES) and trichloro (1H, 1H, 2H, 2H-perfluorooctyl) saline (97%) was ordered from J&K Scientific, USA. The 96% Tween 20 solution (catalog no. T8220) was from Solarbio, China. SARS-CoV-2 spike protein RBD (mFc Tag) (catalog no. ABIN691175) was ordered from antibodies-online, USA. The target protein, anti-SARS-CoV-2 spike RBD neutralizing antibody, human IgG1 (catalog no. SAD-S35) was purchased from Acro biosystems, USA. Pre SARS-CoV-2 human serum (catalog no. 009-000-234, Jackson ImmunoResearch Laboratories INC., USA) diluted (1:50) in the commercial nasal fluid (catalog no. BZ251-0922A, Biochemazone, Canada) was used to simulate the complex mucosal specimen.

For chip fabrication, PDMS (Sylgard TM184) was ordered from Dow Corning, USA. SU8 2015 photoresist was purchased from Gersteltec Sarl, Switzerland. The silicon wafer was bought from Suzhou Crystal Silicon Electronic & Technology Co. Ltd, China. Hydroxy-terminated PDMS (viscosity: 25 cSt; 481939) was from Sigma-Aldrich, USA.

For sampling, the sterile nasal swabs were from Kanmine Co., Ltd, China. The disposable sterile blood collection needle was from Icare Medical Supply Inc., and the glass capillary with 75-μl capacity was from Hirschmann.

1.2 Collection of volunteer specimens

Clinical samples were collected under the Human Subjects Ethics Subcommittee in City University of Hong Kong approved study protocol (ref no.: HU-STA-00000211). Eighty-seven volunteers who received at least two doses of SARS-CoV-2 vaccination were recruited for the collection and informed consent from each volunteer was obtained. The volunteers were required to do a SARS-CoV-2 antigen rapid test before arrival, and those who got negative results were invited for sampling. All materials, including nasal swabs, disposable blood collection needles, tubes, etc, used in the sampling are sterilized. For collection of nasal secretion, the swab was inserted and carefully stirred for 10 s in both the left and right nostrils to stimulate the production of NS. After taking a 10 s break, the swab was again inserted in the nostrils and stirred for 20 s to get enough NS. The swab was weighed before and after sampling to ensure NS weight to be approximately 80 mg (~80 μl). Considering the variance among human subjects, the actual weight was recorded to calculate elution factors defined as (NS weight difference + 120)/NS weight. After sampling, the swabs were immediately inserted in the sterile tube containing 120 μl elution buffer (1% Tween 20 in 1% bovine serum albumin (BSA) solution) and stirred continuously for 3 min to fully elute the secretions. After disposing of the swab in the biological waste bags, the remaining supernatant (NS solution, around 80 μl) was aliquoted in four protein lobind tubes for 20 μl per tube. Finally, the tubes containing NS solutions were marked and stored at -80 ℃ until use. For fingerstick blood collection, A disposable sterile blood collection needle was used to puncture the fingertips to collect 75 μl of finger-prick blood using a glass capillary coated with an anticoagulant. Next, the fingers were wiped with a cotton swab moistened with alcohol and wrapped with an adhesive bandage. The collected blood was transferred into a 500 μl centrifuge tube and centrifuged at 4 ℃, 10500 rpm for 10 min to remove blood cells and isolate the plasma. Lastly, the obtained plasma was marked and stored at -80 ℃ until use.

1.3 Enzyme-linked immunosorbent assay (ELISA) for human sample detection.

The 96-well SARS-CoV-2 IgG ELISA kits (catalog no. K-16027-001, Advansta, USA) targeting spike RBD were used according to the provided protocol. For sample preparation, standard and control samples were created by serial dilutions of anti-spike RBD IgG in model solution and commercial human serum. The unknown human NS samples and plasma samples were diluted 20 times and 250 times respectively with AdvanBlock-EIA solution before use. To prepare the ELISA, a volume of 100 µl of antigen solution prepared by diluting the spike RBD stock solution (200 µg/ml) in 1× EIA coating buffer 100 times was added to each well and incubated at room temperature for one hour. After that, the wells were washed 3 times with 250 µl 1 × AdvanWash Washing Solution. Next, the wells were blocked with 250 µl AdvanBlock-EIA solution for 30 min at room temperature to block spare binding sites. After washing 3 times with 1 × AdvanWash Washing Solution and completely removing the solutions, 50 µl of diluted samples, including the standard samples, controls and unknown volunteer samples were quickly transferred into the assay plate in duplicate and sealed to incubate for another 1h at room temperature. Then, the cover tape was removed and the plate was washed 3 times again, followed by adding 100 µl/well of Anti-IgG horseradish peroxidase (HRP) conjugate and incubate for 30 min at room temperature. After washing the plate 3 times, 100 µl/well TMB substrate solution was added and incubated for 30 min at room temperature in the dark before adding 100 µl/well stop solution. The color of the mixture immediately changed from blue to yellow. After the reaction, the plate was put in a microplate reader (SpectraMax M5e Multi-Mode Microplate Reader, Molecular Devices) to measure absorbance at 450nm.

2. Supplementary figures and tables

Supplementary Figure S1

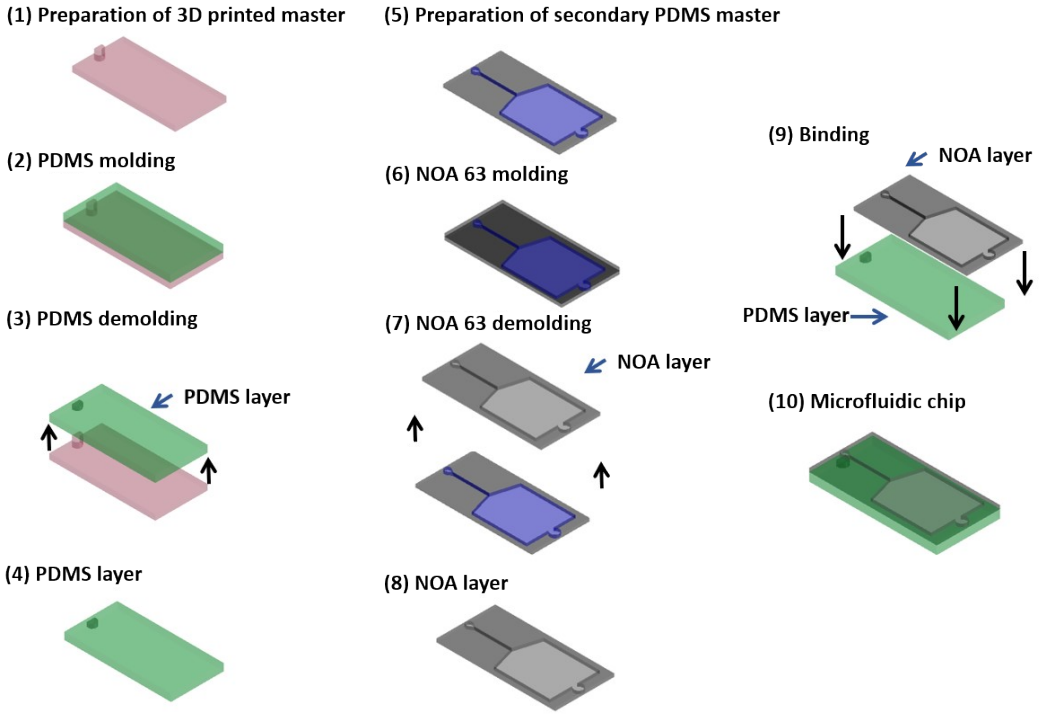

Figure S1. The fabrication process of the PDMS and NOA 63 microfluidic chip. (a) Preparation of the 3D printed mold for PDMS layer. (b) PDMS layer prepared by casting on the 3D printed mold. (c) PDMS layer curing and demolding. (d) The final completed PDMS layer. (e) Secondary PDMS layer prepared by casting on first PDMS that was made with photolithography. (f) NOA 63 molding on secondary PDMS master layer. (g) UV curing, demolding and cutting of NOA 63 layer. (h) The final completed NOA 63 layer. (i) Bonding between PDMS and NOA 63 layer after plasma treatment. (j) The final completed PDMS-NOA 63 microfluidic chip.

Supplementary Figure S2

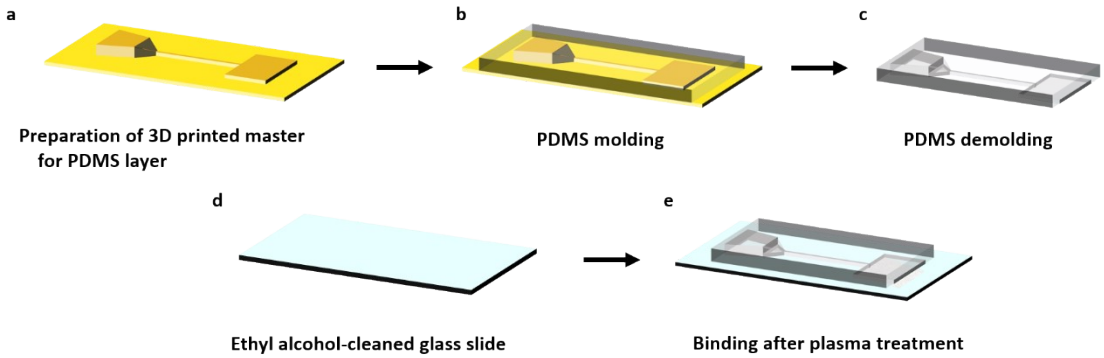

Figure S2. The work steps for fabricating the PDMS and glass microfluidic chip. (a) Preparation of the 3D printed mold for PDMS layer. (b) PDMS layer prepared by casting on the 3D printed mold. (c) PDMS layer curing and demolding. (d) Ethyl alcohol-cleaned glass slide. € The final completed PDMS-glass microfluidic chip bonding between the tape-cleaned PDMS layer and NOA 63 layer after plasma treatment.

Supplementary Figure S3

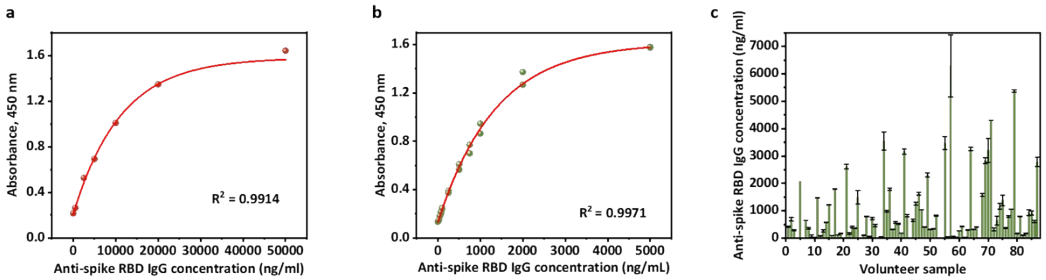

Figure S3. Standard curve of ELISA based on anti-spike RBD IgG spiked in human serum and nasal mucus model solution. (a-c) The non-linear regression equation of ELISA results based on anti-spike RBD IgG spiked in human serum (a): $y = 1.5791 - 1.3685 * e^{-\frac{8.8991}{100000} * x}$, $R^2 = 0.9914$ and nasal secretion model solution (b): $y = 1.6166 - 1.4871 * e^{-\frac{7.3692}{10000} * x}$, $R^2 = 0.9971$. (c): Calculated anti-spike RBD IgG concentration of 87 NS samples based on ELISA (mean ± SD, n = 3).

Supplementary Figure S4

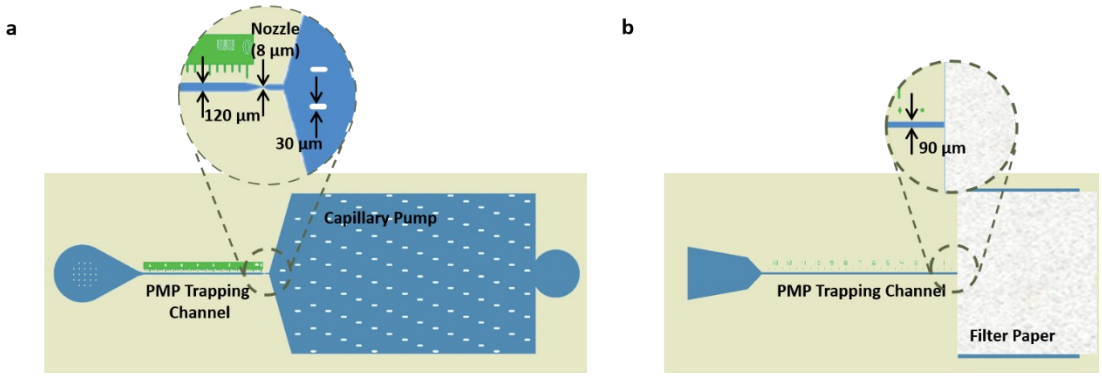

Figure S4. Schematics of PDMS-NOA 63 microfluidic chip with 8 µm nozzle (a) and PDMS-glass microfluidic chip with filter paper (b).

Supplementary Figure S5

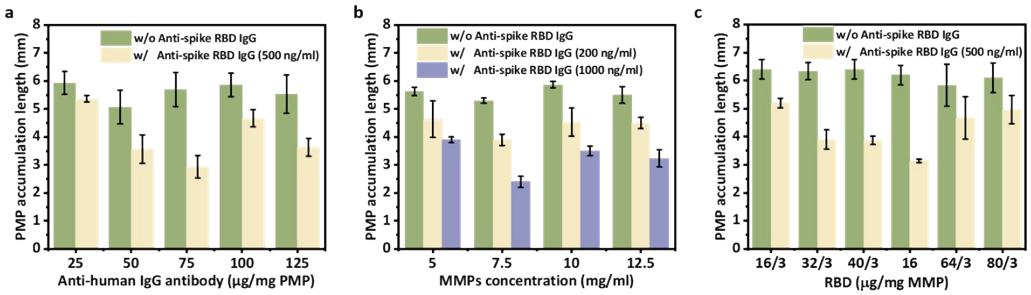

Figure S5. Optimization of MMPs concentration and protein immobilization on microparticles for anti-spike RBD IgG detection in nasal secretion model solution using microparticle microfluidic particle counter system (mean ± SD, n=3). Optimization of (a) anti-human IgG on PMPs (other conditions: 20 mg/ml of PMPs, 7.5 mg/ml of MMPs, $\frac{40}{3}$ μg of RBD per milligram of MMPs), (b) MMPs concentration (other conditions: 20 mg/ml of PMPs, 75 μg of anti-human IgG per mg of PMPs, $\frac{40}{3}$ μg of RBD per mg of MMPs), and (c) RBD on MMPs (other conditions: 20 mg/ml of PMPs, 7.5 mg/ml of MMPs, 75 μg of anti-human IgG per mg of PMPs).

Supplementary Figure S6

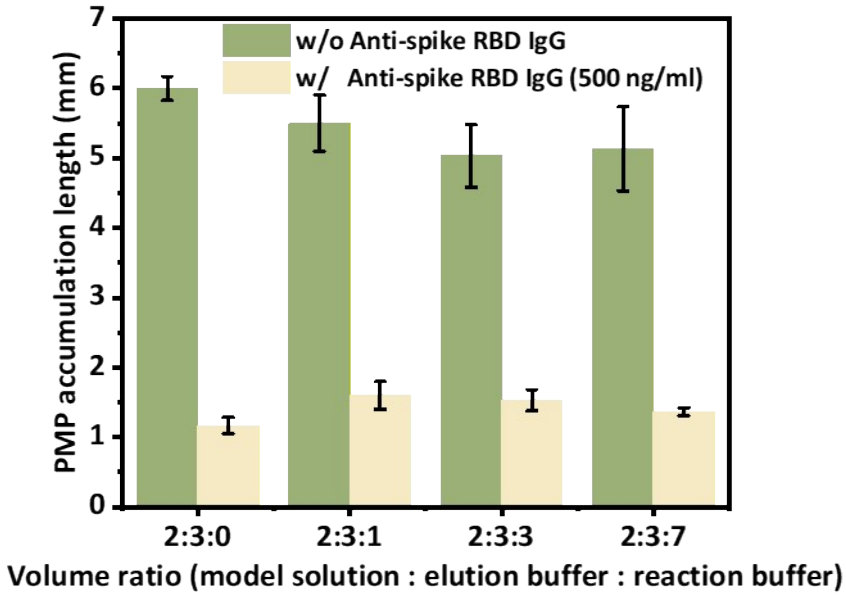

Figure S6. Optimization of volume ratio between model solution, elution buffer and reaction buffer for microfluidic particle counter system (mean ± SD, n=3), explaining the combination effect of viscosity and reaction volume on reaction efficiency. The volume ratio between the model solution and elution buffer was consistent with the ratio used in the human sample collection as approximately 2 : 3 (80 μl : 120 μl).

Supplementary Figure S7

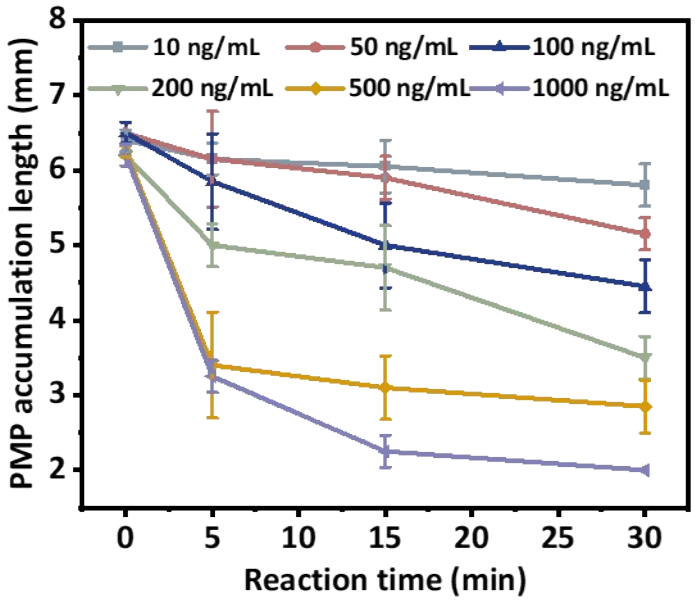

Figure S7. Optimization of reaction time for both first and second incubation of the microfluidic particle counter system (mean ± SD, n=2). The reaction time was optimized by incubating different concentrations of anti-spike RBD IgG in nasal mucus model solution (10, 50, 100, 200, 500, 1000 ng/ml) at (0, 5, 15, 30) min for both first and second incubation.

Supplementary Figure S8

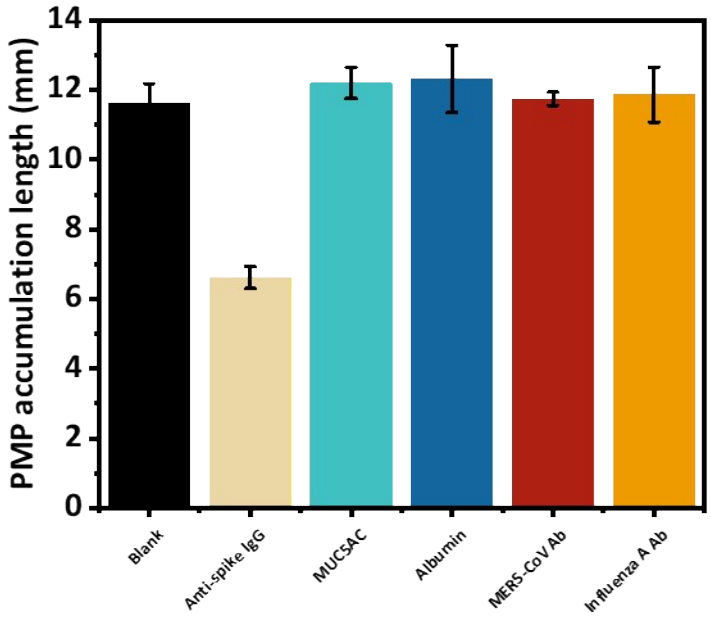

Figure S8. Specificity detection of the system. Measurement of PMP accumulation against other interference with higher concentration (mean ± 95% confidence interval, n = 3).

Supplementary Figure S9

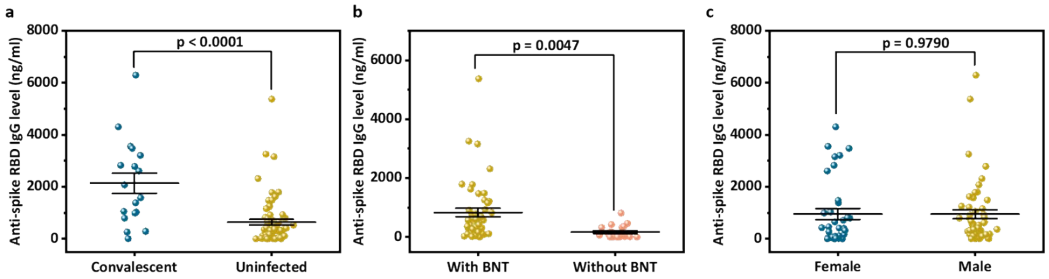

Figure S9. Analysis of level of anti-spike RBD IgG based on infection, gender and vaccine type by ELISA. (a-c) Level of anti-spike RBD IgG in nasal mucus based on infection (a), vaccine type (b) and gender (c).

Supplementary Figure S10

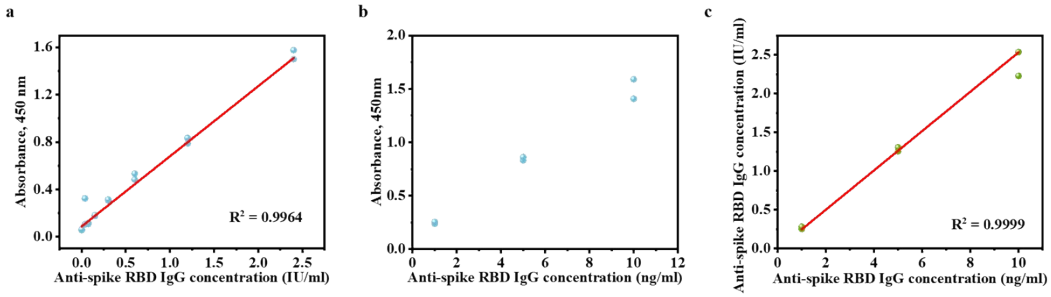

Figure S10. Unit conversion from IU/ml to ng/ml. (a) For the standard solution of concentration from 0 to 2.5 IU/ml, the linear regression equation: $y = 0.0874 + 0.5925 * x$ ($R^2 = 0.9964$). (b) The optical density at the wavelength of 450 nm was obtained using different concentrations of standard solutions in ng/ml (1, 5, 10 ng/ml). (c) For unit conversion of anti-spike RBD IgG from ng/ml to IU/ml, the linear regression equation: $y_{(IU/ml)} = -0.0056 + 0.2538 * x_{(ng/ml)}$ ($R^2 = 0.9999$). Based on the conversion equation, the protection threshold of 645 IU/ml equals to 2541.5 ng/ml.

148 **Table S1.** The acronyms and the corresponding full names

Acronyms	Full names
SARS-CoV-2	Severe Acute Respiratory Syndrome Coronavirus 2
COVID-19	Coronavirus Disease 19
RBD	Receptor Binding Domain
LOD	Limit of Detection
S Protein	Spike Protein
MMPs	Magnetic Microparticles
PMPs	Polystyrene Microparticles
IgG	Immunoglobulin G
Anti-spike RBD IgG	IgG Antibody against SARS-CoV-2 Spike Protein Receptor-Binding Domain
Anti-human IgG	Secondary Antibody against Human IgG
S-specific IgG	IgG Antibody against Spike Protein
S1 RBD	Spike1 Protein Receptor-Binding Domain
N-specific subgenomic RNA	Specific Subgenomic Ribonucleic Acid of Nucleocapsid Protein
ACE2	Angiotensin-converting Enzyme 2
ELISA	Enzyme-Linked Immunosorbent Assay
POCT	Point-of-care Testing
LFIAs	Lateral Flow Immunoassays
BSA	Bovine Serum Albumin
NS	Nasal Secretion
PBS	Phosphate Buffered Saline
MUC5AC	Mucin-5AC
MERS-CoV	Middle East Respiratory Syndrome Coronavirus
EDC	1-ethyl-3-(3-dimethylaminopropyl)carbodiimide Hydrochloride
NHS	N-hydroxysuccinimide
MES	2-(N-Morpholino)ethanesulfonic Acid
PDMS	Polydimethylsiloxane
HRP	Horseradish Peroxidase
OD450	Optical Density at the Wavelength of 450 nm
NOA63	Norland Optical Adhesive 63
3D-Printing	Three-dimensional-printing
UV	Ultraviolet
HMDS	Hexamethyldisilane
CVD	Chemical Vapor Deposition

149

3 Data processing and analysis

3.1 Linear regression

In a linear model, $y = b_0 + b_1 x$ was considered to perform least-squares regression, where y is the dependent variable, representing the predicted result for a given independent variable, x. In this study, the model is used in both sensitive and rapid modes, while y represents the PMP accumulation length of the microfluidic chip and x is the anti-SARS-CoV-2 spike RBD IgG concentration. The constants applied in the calculating formula including the estimates of the intercept b_0, the slope b_1, their variances $s_{b_0}^2$, $s_{b_1}^2$ and the residual variance of the regression $s_{\frac{y}{x}}^2$ were determined with the below equations:

$$b_0 = \bar{y} - b_1 \bar{x} \quad (1)$$

$$b_1 = \frac{\sum_{i=1}^{n} (x_i - \bar{x}) y_i}{\sum_{i=1}^{n} (x_i - \bar{x})^2} \quad (2)$$

$$s_{b_0}^2 = s_{\frac{y}{x}}^2 \left(\frac{1}{n} + \frac{\bar{x}^2}{\sum_{i=1}^{n} (x_i - \bar{x})^2} \right) \quad (3)$$

$$s_{b_1}^2 = \frac{s_{\frac{y}{x}}^2}{\sum_{i=1}^{n} (x_i - \bar{x})^2} \quad (4)$$

$$s_{\frac{y}{x}}^2 = \frac{\sum_{i=1}^{n} (y_i - \hat{y}_i)^2}{n - 2} \quad (5)$$

Where x_i (anti-SARS-CoV-2 spike RBD IgG concentration) and y_i (PMP accumulation length) are the paired data got from the experiments, n is the total number of data points calculated by $n = \sum_{j=1}^{k} m_j$, k is

the number of concentration levels, m_j is the times of repetition at each concentration level, $\bar{x}$ and $\bar{y}$, is the mean value of x_i and y_i, as shown below:

$$\bar{x} = \sum_{i=1}^{n} \frac{x_i}{n} \quad (6)$$

$$\bar{y} = \sum_{i=1}^{n} \frac{y_i}{n} \quad (7)$$

And $\hat{y}_i$ is the predicted value of y for a particular concentration x_i, as shown in equation:

$$\hat{y}_i = b_0 + b_1 x_i \quad (8)$$

Hence, the calibration curve is expressed as:

$$y = b_0 + b_1 x \pm t_{(\alpha, n-2)} s_{\frac{y}{x}} \left(\frac{1}{m} + \frac{1}{n} + \frac{(x - \bar{x})^2}{\sum_{i=1}^{n} (x_i - \bar{x})^2}\right)^{\frac{1}{2}} \quad (9)$$

Where $t_{(\alpha, n-2)}$ is the critical value of student t distribution, which is selected as 1.645 for the 90% confidence interval of two-tailed hypothesis (α = 0.05), and $\frac{1}{m}$ is the contribute of uncertainty from the average of m replicates in future observation[1, 2].

3.2 Limit of Detection (LOD)

For the estimation of the limits of detection x_D, a non-central t-distribution model is selected with the equation:

$$x_D = \delta_{(\alpha, \beta, n-2)} \frac{s_{\frac{y}{x}}}{b_1} \left(1 + \frac{1}{n} + \frac{\bar{x}^2}{\sum_{i=1}^{n} (x_i - \bar{x})^2}\right)^{\frac{1}{2}} \quad (10)$$

Where $\delta_{(\alpha, \beta, n-2)}$ is the non-centrality value of the non-central t-distribution taking protection against both type I error rate (α, false-positive) and type II error rate (β, false-negative)[1, 2]. The other constant

182 variances were calculated the above equations. All LOD was determined based on an appropriate linear
183 range evaluated by the R^2.

184 **3.3 Accuracy**

185 The measured antibody level by microfluidic chip (Y) is compared with that by the gold standard
186 method ELISA (X) to study the accuracy. The agreement between two sets of measured antibody levels
187 of the 74/84 volunteers' nasal mucus samples is quantified using Lin's concordance correlation
188 coefficient ($\hat{\rho}_C$), as shown below:

189
$$\hat{\rho}_C = \frac{2\rho\sigma_x\sigma_y}{(\mu_Y - \mu_x)^2 + \sigma_Y^2 + \sigma_X^2} \qquad (11)$$

190 Where μ_Y and μ_x are the means, σ_Y^2 and σ_X^2 are the variances, and ρ is Pearson's correlation coefficient[3].

Reference

(1) Clayton, C. A.; Hines, J. W.; Elkins, P. D. Detection limits with specified assurance probabilities. *Analytical Chemistry* **1987**, *59* (20), 2506-2514.

(2) Lavagnini, I.; Magno, F. A statistical overview on univariate calibration, inverse regression, and detection limits: Application to gas chromatography/mass spectrometry technique. *Mass spectrometry reviews* **2007**, *26* (1), 1-18.

(3) Lawrence, I.; Lin, K. A concordance correlation coefficient to evaluate reproducibility. *Biometrics* **1989**, 255-268.